

Thermal Design and Analysis of the Mars Exploration Rover Surface Impact Airbags

D. K. Harris,* D. C. Wilson,[†] and J. Rade[‡]
Auburn University, Auburn, Alabama 36849-5341

DOI: 10.2514/1.16782

The design of the Mars Exploration Rover surface impact airbags is described along with a thermal finite differencing model that was created and benchmarked to predict the internal gas temperature and pressure profiles within the airbags. The airbag system deployed on the Mars Exploration Rover missions was part of the landing system of Mars Pathfinder heritage that cushioned the rover's impact landing onto the Mars surface for impact velocities of up to 24 m/s. The model predicted the internal gas temperatures and pressures for both hot and cold mission landing scenarios. These predictions were used to help define the boost grain propellant loading needed within the gas generators in order to produce the necessary internal airbag gas pressure. Predictions of the amount of condensation created within the airbags during and after inflation proved to be the most crucial influence on the internal bag pressure. Final mission predictions for the airbag internal pressures are presented for both hot and cold landing scenarios.

Nomenclature

A	=	area
c_v	=	constant volume specific heat
Gr	=	Grashof number
g	=	gravitational constant
h	=	convection coefficient
\bar{h}	=	average convection coefficient
h'_{fg}	=	enthalpy of evaporation
k_l	=	liquid thermal conductivity
$L_{\text{effective}}$	=	effective length
m	=	mass
\dot{m}	=	mass flow rate
Nu	=	Nusselt number
P	=	pressure
P_{CO_2}	=	CO ₂ gas pressure
$P_{\text{H}_2\text{O}}$	=	H ₂ O vapor pressure
Pr	=	Prandtl number
Q	=	heat transfer
Re	=	Reynolds number
T_{sat}	=	saturation temperature
T_{surface}	=	surface temperature
t	=	time
u	=	internal energy
v	=	velocity
V_{bag}	=	airbag volume
Δ	=	difference or change
$\epsilon_{\text{effective}}$	=	effective emittance
ρ	=	density
σ	=	Stefan–Boltzmann const
∞_l	=	liquid viscosity

GG	=	gas generator
L	=	based on length
ℓ	=	liquid
v	=	vapor

Introduction

IN June and July of 2003 NASA separately launched onboard Boeing Delta II rockets two mechanical Mars rovers designated as Opportunity and Spirit. This interplanetary exploration program, known as MER A & B, was managed out of NASA's Jet Propulsion Laboratory (JPL). The landing system used on the Mars Exploration Rover (MER) vehicles included parachutes, retrorockets, and external airbags to absorb the impact of the landing event. Although this system had flight heritage from the Mars Pathfinder Program the MER missions comprised an increase in landing mass by an order of magnitude. The airbags were inflated approximately 6 s before impact with the Mars surface with a vehicle velocity of up to 24 m/s. The shock experienced by the system was estimated to be the equivalent of up to 40 gravitational equivalents. Upon impact the vehicle was expected to bounce over the Mars surface for about 1 min spanning up to a mile. The vehicle was expected to bounce about every 3 to 5 s before coming to rest. The airbags were used to cushion the impacts and absorb the vehicle's kinetic energy. Airbag integrity had to be assured over the entire impact sequence. The airbags needed an internal pressure as specified by JPL mission analysts of $1.0 \pm 0.0 / -0.1$ psi. The airbags also had to survive abrasion threats caused by encounters with sharp rock formations. The airbag design features concerning external threats are outside the scope of this paper. The two modes of airbag failure considered were overpressurization and stroke-out. The first mode would result in a catastrophic failure, and the second mode would involve an impact with the Mars surface. The second mode would not constitute a catastrophic failure but would most likely damage the rover and threaten mission success. Although the vehicle was expected to experience over 20 bounces during the landing impact sequence it was determined by JPL mission analysts that only the first several bounces were most critical. It was decided that the first 6 s of bouncing were most crucial for the airbags and that there was a large margin of safety after that point.

Three ATK built gas generators delivered exhaust gases into four airbags surrounding the vehicle just before impact. The four airbags included three petal (side) airbags and one base airbag. All three side bags had an ATK gas generator. The base petal had no gas generator and received its hot gases from all three petal airbags via a vent port between the base airbag and each of the three side petal airbags. Just

Subscripts

amb = ambient

Received 23 March 2005; revision received 24 April 2006; accepted for publication 11 October 2006. Copyright © 2006 by the American Institute of Aeronautics and Astronautics, Inc. All rights reserved. Copies of this paper may be made for personal or internal use, on condition that the copier pay the \$10.00 per-copy fee to the Copyright Clearance Center, Inc., 222 Rosewood Drive, Danvers, MA 01923; include the code 0022-4650/07 \$10.00 in correspondence with the CCC.

*harridk@auburn.edu (corresponding author).

[†]Engineer, current address: ILC Dover, One Moonwalker Road, Frederica, DE 19946-2080; wilsod@ilcdover.com.

[‡]Engineer, current address: ATK Advanced Propulsion and Space Systems Group, Elkton, MD 21922; james.rade@atk.com.

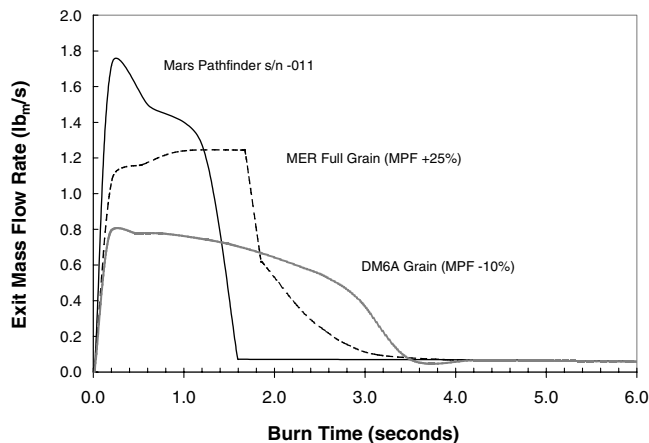


Fig. 1 Mass injection profiles comparison between MPF heritage and MER.

before impact all three generators were fired causing the airbags to inflate within a required 3 s time frame. The generators burned through the boost grain and most of the coolant pellets in about 3 s. The sustain grain burned from ignition up to about 22 s. The average grain loadings for all gas generators used in Mars Pathfinder was 1312.6 g, while that for both flight ship sets for MER A&B averaged 1392.7 g. Figure 1 shows the mass injection profiles computed by ATK (gas generator subcontractor) for both the Mars Pathfinder (MPF) and the two extreme grain loading cases considered for MER, which included a -10% and $+25\%$ boost grain loading from MPF boost grain. The sustain grain chamber and loading were identical to that used in the Mars Pathfinder for all designs considered for MER. As can be observed in the profiles most of the grain mass is injected into the airbags within 3 s and all grain loadings have an identical sustain grain burn profile.

System Design and Modeling

A finite difference thermal model of the airbag landing system was created for the Mars Exploration Rover mission similar to the model created for the Mars Pathfinder mission as described in [1]. The model was created using GSINDA of Network Analysis, Inc. The purpose of creating this thermal temperature and pressure model (heretofore referred to as the T&P model) was to determine the pressure inside the four airbag landing system developed by ILC, Dover, using gas generators built by ATK Tactical Systems of Elkton, Maryland. The mass injection and thermal and kinetic energy profiles for the gas generators were provided by ATK and are shown in Figs. 2 and 3. The gas injection velocity profile has a distinct plateau indicating a choked flow condition. Each airbag had an internal volume of about 11.5 m^3 and an internal surface area of about 30.428 m^2 . Bag construction consisted of two internal layers and six abrasion outer layers. The internal layers (consisting of a

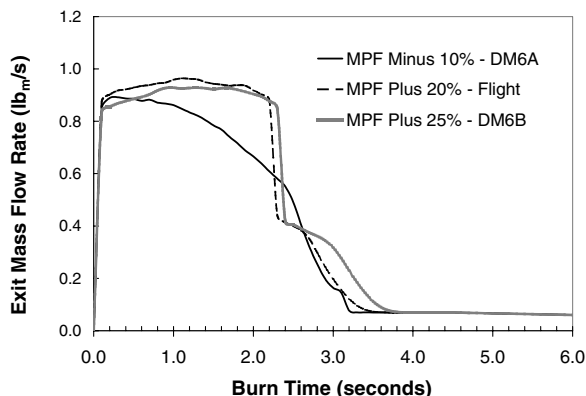


Fig. 2 Gas generator mass injection profiles.

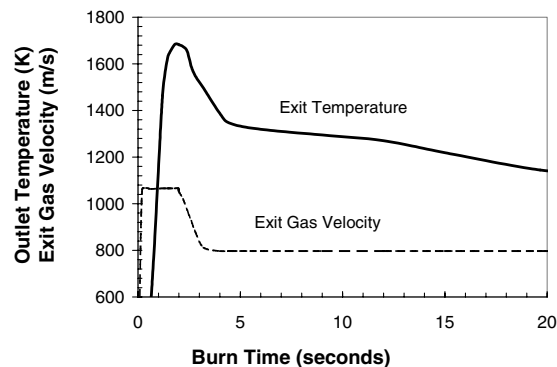


Fig. 3 Gas generator thermal and kinetic energy injection profiles.

bladder and a restraint layer) were constructed using Vectran coated with silicone. The abrasion layers were constructed using uncoated Vectran. Table 1 shows the airbag system properties used for modeling purposes. The airbag fabric layer masses and the tendon masses given in Table 1 were adjusted in the GSINDA models (described later) to match transient temperature profiles observed during bag inflation tests. There are two reasons why the fabric masses had to be modified for the model. The first reason is that there are dense layers at the fabric seams where there is a significant buildup of resin for structural integrity. The second reason is the modeling method used where a single diffusion node represented each fabric layer. The adjustments made were necessary because the model assumed a single bulk-averaged fabric layer temperature, whereas any measurements made during testing represented a single local temperature reading made at a convenient location, which may not represent the layer average temperature. Also present in the airbag system are load-bearing tendons, both internal and external. The internal tendons are represented in the model as a single diffusion node connected only to the internal gases via convection and radiation. Finally, the two extreme environmental landing scenarios considered for MER mission predictions are summarized in Table 2. The nominal case landing scenario (not shown) is taken as the average (or midpoint) between the hot and cold cases.

Model Requirements, Assumptions and Limitations

The utility and purpose of the T&P model was to determine the grain loading necessary within the ATK gas generators to achieve a nominal $1.0 + .0 / - 0.1$ psi gage bag pressure within the airbags for the first several impacts on the Mars surface. Also, the model was used to estimate the expected range of airbag pressure at impact based upon hot and cold mission landing scenarios; that is, the sensitivity of initial fabric temperatures and Mars environmental parameters on air pressures was needed. Also of great interest

Table 1 Airbag assembly and material properties

<i>System mass, volume, and area summary</i>	
Volume	11.5 m ³
Bladder layers	6.83 kg
Abrasion layers	9.3 kg
Internal surface area	30.428 m ²
External surface area	24.7533 m ²
Lander contact area	0.908 m ² (petal airbag) 1.106 m ² (base airbag)
<i>Dimensions</i>	
Internal tendon lengths	16.5 side (20.803 m with splices) 15.494 m bottom (18.695 m with splices)
Airbag assembly	5.2 m diam sphere
Internal vents	0.166 m ² per vent
<i>Mass summary (single airbag except as noted)</i>	
Airbag total mass	21.5 kg
Bladder mass	6.83 kg
Abrasion layers	9.025 kg
Internal tendons	0.514 kg (petal airbag) 0.462 kg (base airbag)

Table 2 MER mission hot and cold mission scenarios

	Cold mission	Hot mission
Fabric emissivity	0.85	0.85
External convection	20 W/m ² · K	10 W/m ² · K
Lander temperature	−25°C	0°C
Initial bag temperature	−45°C	−25°C
Mars sky environment	−163°C	−123°C
Mars soil environment	−23°C	−3°C
Mars atmospheric temperature	−60°C	−20°C
Solar flux	450 W/m ²	550 W/m ²
Ambient pressure	5 torr (650 Pa)	5 torr (650 Pa)

was the prediction of the amount of moisture condensation within the airbags. It was found from modeling that the amount of condensation present would greatly influence the internal bag pressures. There was a significant amount of water created by the gas generator's propellant and the specific volume of water vapor is 1000 times greater than that of liquid water. Therefore, the range of internal bag pressures possible from condensation alone was greater than the model accuracy depending on the amount of water condensed. Because this parameter could not be directly measured or observed it was estimated from the model output.

The limitations and assumptions imposed on the model and its results were 1) bag pressure accuracy is $\pm 5\%$, 2) gas temperature accuracy is $\pm 5\%$, 3) any influences from impacts with the Mars surface are not directly modeled, 4) all petal airbags are uniform in pressure and temperature, 5) internal gases are an ideal gas mixture, 6) gas kinetic and potential energies are negligible compared to the internal energy of the gas mixture inside the airbags, 7) the effects of gas thermal gradients within each bag are ignored, 8) the external tendons do not influence the internal gas temperatures, 9) each fabric layer and the bladder and restraint layers are represented by separate single diffusion nodes, 10) the temperature for all airbag fabric layers is assumed isothermal within the specific layer, 11) the airbag volume opens in a linear fashion and is fully deployed within 1.5 s, 12) the model predictions during the inflation are not intended to represent the actual bag inflation dynamics, 13) the lander remains at a constant temperature during the entire 80 s time duration under concern, and 14) the lander is spinning at such a rate as to allow the external Mars radiation environment to be modeled as isotropic.

Relevant Heat and Mass Transfer Processes

The internal airbag pressure depended on the molar amount and temperature of the gas injected by the gas generators. The temperature of the internal airbag gases depended on the heat transfer between the gases and the internal bladder surface. The three modes of heat transfer include natural and forced convection, and radiation. While natural convection occurs during the entire 80 s of analysis, forced convection occurs only during the period during and immediately following the mass injection from the gas generators. The swirling gases invoke a forced convection component to the heat transfer that decays in about 3–5 s after the end of the sustain grain burn (at about 22 s after inflation).

Internal Forced Convection

Forced convection is represented in the model using the following correlation, found in [2,3],

$$Nu = 0.664 \cdot Re^{1/2} Pr^{1/3} \quad Re_L < 5 \times 10^4$$

$$Nu = 0.036 \cdot Pr^{1/3} (Re_L^{0.8} - 23,200) \quad Re_L \geq 5 \times 10^4 \quad (1)$$

The Reynolds number is based upon a swirl velocity similar to that used in the Mars Pathfinder model [1] as shown here,

$$V_{\text{swirl}} = \frac{6 \cdot V_{\text{GG,exit}}}{L_{\text{effective}}} \sqrt{0.00050671} \quad (2)$$

In Eq. (2) the velocity term is the gas velocity at the gas generator exit, as provided by ATK, and the effective length is defined as the internal airbag volume divided by the internal airbag surface area.

Internal Natural Convection

The natural convection currents were modeled using the following general Nusselt number behavior shown in Eq. (3),

$$Nu = C \cdot (Gr \cdot Pr)^m \quad (3)$$

The values of C and m have the values of 0.13 and 0.333 for the initial inflation event. These values were obtained in the work by Ulrich et al. [4]. However, according to their observations, the effect of injecting gases was short lived: only 3–4 s after the end of injection. Therefore, at the end of the gas generator's propellant burn (at about 22 s after inflation), the constants were forced in an exponentially decaying fashion to the more nominal values of 0.228 and 0.226, for C and m , respectively. These values are for gases or liquids within a spherical annulus and were reported by Weber et al. [5].

Combined Effects

The combined forced and natural convection effects were handled as is commonly found in the heat transfer literature [2,3] as follows:

$$Nu = \sqrt[3]{Nu_{\text{free}}^3 + Nu_{\text{forced}}^3} \quad (4)$$

Internal Gas Radiation

The internal gaseous radiation calculations were accomplished using Leckner's correlations [6] of Hottel's measurements for both carbon dioxide and water. The band overlapping was also accounted for in these correlations. The general forms of the correlations were as follows in Eqs. (5) where the coefficients for both water and carbon dioxide are given in [6]:

$$l_n \varepsilon_o = a_o + \sum_{i=1}^M a_{i\lambda^i} \quad \text{with} \quad a_i = c_{oi} + \sum_{j=1}^M c_{ji} \tau^j \quad (5a)$$

$$\zeta = \frac{P_{\text{H}_2\text{O}}}{P_{\text{H}_2\text{O}} + P_{\text{CO}_2}} \quad \Delta \varepsilon = \left\{ \frac{\zeta}{10.7 + 101\zeta} - 0.0089\zeta^{10.4} \right\} \cdot \lambda^{2.76} \quad (5b)$$

Internal Moisture Condensation

One of the main concerns for the airbag landing system addressed by this model was the process of water condensation because water was a significant byproduct of the gas generator's propellant. The amount of water in the products of combustion by the gas generators was around 36%. The amount of water condensed on the bladder surface influenced the amount of moles of water vapor inside the airbags and, hence, the internal gas pressure. Two main issues regarding the level of accuracy for the condensation calculations existed. First, it was necessary to have a reliable estimate of the amount of water generated by the combustion of the ATK propellant inside the gas generators. The percentage of water generated was empirically determined at ATK during a lot acceptance test (LAT). Second, the accuracy of the T&P model's condensation computations needed to be verified. This concern was handled during the benchmarking process by comparing pressure predictions to measurements during thermal vacuum inflation testing in addition to LAT tests. The latter of these tests was useful because no condensation occurred inside the altitude tank at ATK by virtue of the tank being held above the dew point. The equation used to compute the heat transfer coefficient associated with condensation in the MER T&P model is that described in [7],

$$Nu_L = \frac{\bar{h}_L L}{k_l} = 0.943 \left[\frac{\rho_l g (\rho_l - \rho_v) h'_{fg} L^3}{\mu_l k_l (T_{sat} - T_{surface})} \right] \quad \text{and} \quad (6)$$

$$q = \bar{h}_L A (T_{sat} - T_{surface})$$

However, this correlation is for condensation in the presence of pure water vapor. A correction had to be added for the presence of noncondensable gases, as is the case for the airbag analyses. The corrections applied are found in [7] where the dependence is upon the specific humidity of the condensing vapor. For the MER airbag system a significant reduction in the amount of condensation was realized due to a high level of noncondensable gases.

Interstitial Layer Thermal Resistance

The interstitial thermal resistance between the fabric layers was modeled by linear conductance in the GSINDA model that was adjusted from thermal vacuum inflation test data. The radiation (or nonlinear) heat transfer between layers was not considered significant due to the nature of the fabric surfaces and the small temperature differences between fabric layers.

External Convection

The convective thermal connection between the airbag fabric and the Mars atmosphere was computed based upon a lander velocity of 24 m/s and an equivalent diameter of 2.33 m for the entire airbag system (all four airbags). The resulting Reynolds number for the Mars atmosphere was 7.7×10^6 , giving a Nusselt number of 3088, which gave a convection coefficient number of $20.0 \text{ W/m}^2 \cdot \text{K}$. The outer abrasion layer surface area that was exposed to the Mars atmosphere was 24.753 m^2 .

External Radiation

Radiation between the outer abrasion layers and the Mars sky and surface environment was computed using a simple gray surface assumption, Eq. (7),

$$Q = \sigma \varepsilon_{\text{effective}} A_{\text{airbags}} (T_{\text{Airbags}}^4 - T_{\text{Mars}}^4) \quad (7)$$

In Eq. (7) the area is the exposed area for the external abrasion layer (19.669 m^2) and the temperature of the Mars environment is the average of the sky and surface temperatures because the lander is rotating and no preferred attitude is being maintained before impact. The effective gray surface emissivity for the external fabric layer was set at 0.85. Finally, the albedo (reflected UV off the Mars surface) was also included in the model at a value of 0.3.

Model Nodal Philosophy

The GSINDA model contained a representation of one petal bag connected to the base bag. It was determined that symmetry among the three petal bags existed due to the uniformity of the outer Mars environment. Therefore, one gas generator was fed into the petal bag, which in turn vented into the base bag. During actual thermal vacuum testing it was always observed that the base bag gases were about 100°C cooler than the petal bag gas. Because the bags were always close to uniform in pressure, as would be expected, this indicated that the base bag always contained more gas mass than the petal bags, on average. That is, although the thermal diffusion process is slower and gives rise to a cooler base bag gas and fabric temperature, the acoustic speed at which pressure information travels gives rise to an almost instantaneous pressure equilibration among the bags. This was consistently observed in three full-system inflation tests: Mars Pathfinder qualification and both the MER thermal vacuum inflation tests reported in this paper. The model also contained logic to account for venting between the base bag and the other two petal bags that mimicked exactly the venting that occurred between the petal bag and the base bag in the real airbag system. That is, it was assumed that the venting to and from the base bag was identical for all three petal bags at any instant in time. This assumption was corroborated by inspections of full-system inflation data. The airbag venting was

Table 3 Airbag system leakage rate per bag-to-ambient pressure differential

MPF design		MER design set A		MER design set B	
ΔP , Pa	m^3/s	ΔP , Pa	m^3/s	ΔP , Pa	m^3/s
1793	0.0335	1586	0.0205	1379	0.0456
3447	0.0495	3654	0.0425	2137	0.0568
5340	0.0605	5206	0.0444	4964	0.0875
8687	0.0778	7033	0.0533	7584	0.1111

modeled using Eq. (8), where the venting rate is controlled with the values of the constant C . A value of 0.03 was used, which gave good agreement with data while not causing convergence or stability problems in the model,

$$\dot{m} = CA \sqrt{2\rho\Delta P} \quad (8)$$

The overall conservation for all of these processes for the airbag system is given in Eq. (9). The internal energy of the airbag gas is conserved based on the thermodynamic work and heat interactions with the surroundings (i.e., the bladder layer) in the presence of mass losses due to bag leakage. The GSINDA model worked on this conserved property (internal energy) through the property of temperature by virtue of the relationship between internal energy and temperature for an ideal gas, $u = c_v T$,

$$\dot{Q}_{\text{gas}} = \dot{m}_{\text{GG}} \left(h_{\text{GG}} - \frac{v_{\text{GG}}^2}{2} \right) - (\dot{m}_{\text{vent}} + \dot{m}_{\text{leak}}) h_{\text{gas}} - (m_{\text{gas}} u_{\text{gas}})|^{t+\Delta t} + (m_{\text{gas}} u_{\text{gas}})|^t - P_{\text{amb}} \frac{dV_{\text{bag}}}{dt} \quad (9)$$

The leakage through the airbag system was modeled using leakage rate data provided by ILC. A correction factor was included in the model because there could be a difference in the measurements made by ILC at lab pressures and the behavior which would be experienced on Mars, for example, choked flow effects through the microscopic pores of the airbag fabric or sealing effects due to condensate on the bladder surface. This adjustment was verified by comparing the pressure profile during thermal vacuum inflation tests 40–60 s after inflation. During this period of testing the pressure profile was attributed solely to airbag leakage after correcting for thermal effects on the internal pressure. The airbag leakage measurements provided by ILC for both the MPF and MER flight design airbags are given in Table 3. In Table 3 the first column represents data taken at ILC on an original flight design inherited from Mars Pathfinder. However, significant changes in the airbag outer abrasion layer design were made since MPF. These design changes allowed for the MER airbags to have a tighter seal as can be seen by comparing the third and fourth columns (labeled set A) to the first and second columns in the table. Therefore, the set A test article airbags best represented MER flight bags for leakage behavior. The fifth and sixth columns in Table 3 show the air leakage for the set A airbags after considerable rework was completed after many drop tests were performed using those same airbags. The bags (then labeled set B) were reworked for a second full-system thermal vacuum inflation test at Plum Brook Station in early December 2002. The only use for columns five and six was for benchmarking the T&P model to the data from the December 2002 full-system inflation test.

Gas Constituent Analyses

The exact constitutive makeup of the hot exhaust gases needed to be determined in order for the model to accurately predict the internal pressure developed inside the airbag system as the gas generators were fired. Specifically, the percentage of water generated was of great concern due to its capacity to condense into liquid, thereby reducing the amount of gas moles available for internal airbag pressure. Also of interest was the state of oxidation of carbon. The percentage of carbon present as CO as opposed to CO_2 directly affects the amount of oxygen remaining to combine with hydrogen

Table 4 ATK gas generator emission products predictions

Constituent	Mol wt	Mol per 100 grams exhaust product ^a				Total ^b	
	g/mol	A	B	C	D	(g)	%
CH ₄	16.0	0.324	0.520	0.092	0.075	54.4	4.2
CO	28.0	0.000	0.000	0.418	0.572	98.8	7.7
CO ₂	44.0	0.347	0.541	0.837	0.799	336.3	26.2
FeCl ₂	126.8	0.000	0.000	0.001	0.001	0.0	0
HCl	36.5	0.171	0.223	0.654	0.654	188.8	14.7
H ₂	2.0	0.006	0.078	1.454	1.567	17.8	1.4
H ₂ O	18.0	2.279	1.893	0.568	0.490	388.7	30.3
N ₂	28.0	0.612	0.638	0.334	0.334	198.5	15.5
P ₄ O ₆	219.9	0.001	0.001	0.001	0.001	0.0	
C (solid)	12.0	1.010	0.621	0.279	0.180		
FeCl ₂ (solid)	126.8	0.000	0.000	0.000	0.000		
NH ₄ Cl (solid)	53.5	0.052	0.000	0.000	0.000		
Total		4.802	4.514	4.546	4.672	1283.3	100

^aA: Boost grain with coolant while bag inflates, 0.0–1.60 s.^bB: Boost grain with coolant after bag inflation, 1.60–1.80 s.

C: Boost grain without coolant after bag inflation, 1.80–2.0 s.

D: Sustain grain without coolant after bag inflation, 2.0–20.2 s.

^bTotal of gaseous emission products only.**Table 5 FTIR gas analysis performed by ATK**

	Sample cylinder B-3	Sample cylinder B-4
Gas sampling interval	$T + 1 - T + 20$ s	$T + 5 - T + 20$ s
Carbon dioxide (CO ₂)	$5.7 \pm 0.4\%$	$5.3 \pm 0.4\%$
Carbon monoxide (CO)	$25.1 \pm 1.1\%$	$28.0 \pm 1.3\%$
Methane (CH ₄)	$4.8 \pm 0.1\%$	$5.0 \pm 0.4\%$
CO ₂ /CO ratio	0.23	0.19
Ethylene (C ₂ H ₄)	<5%	<5%
Acetylene (C ₂ H ₂)	<5%	<5%
Hydrogen cyanide (HCN)	<0.5%	<0.5%
Hydrogen chloride (HCl)	Trace	<1%
Ammonia (NH ₃)	Not detected	Not detected
Nitrous oxide (N ₂ O)	Not detected	Not detected

Table 6 Permanent gases GC (gas chromatography) analysis performed by JPL

Gas	Calibration std. reported concentration (vol %)	Sample reported concentration (vol %)	Sample with dilution factor $\times 800/450$ (vol %)
Nitrogen	7.6%	$29.7 \pm 1\%$	53.0%
Carbon monoxide	9.7%	$17.5 \pm 0.5\%$	31.0%
Methane	39.7%	1.8%	3.2%
Carbon dioxide	41.0%	3.8%	6.7%
Oxygen/argon	2.0%	1.1%	2.0%
Total	100%	54%	96%

for water creation. The ratio of CO to CO₂ present in the combustion products therefore influenced the amount of water creation possible.

To understand the chemistry of the combustion products a numerical analysis was performed by ATK using a ballistics code developed at NASA Lewis. The results of these numerical simulations gave some interesting insights into the nature of the combustion products of the gas generators. According to the results in Table 4 water was the most abundant combustion product, followed by carbon dioxide. This is an important finding for the model since both gaseous H₂O and CO₂ are participatory in thermal radiation. Also of note was the high amount of HCl, which can go into solution with any condensed water present. Of interest also was that of any carbon in solid phase (i.e., soot) would not be available for CO or CO₂ production. Presence of any soot indicated a significant reduction in the number of gas moles present inside the airbag volume.

In an effort to assess the accuracy of the ballistics model's results in Table 4 two independent gas analyses were conducted by JPL and ATK. ATK analyzed the composition of sample gases collected during a static LAT by using Fourier transform infrared spectroscopy (FTIR). The concentrations of carbon dioxide, carbon monoxide, and methane were determined along with the qualitative presence of the other infrared active gases observed. The results are

summarized in Table 5. The infrared inactive gases hydrogen and nitrogen, which are known to be present in significant concentrations, were not detectable by FTIR. In addition, a bulk gas composition analysis was carried out at JPL using gas chromatography on sample gases taken during the single bag inflation test at Plum Brook on 14 September 2001. The results are shown in Table 6 where the values in the last column are the most relevant to the model. The results summarized in both Tables 5 and 6 confirm the inaccuracy of the NASA Lewis ballistics code results shown in Table 4 with regards to the amount of CO and CO₂ present. There was a significantly larger amount of CO present than predicted indicating that more oxygen molecules were available for water creation than predicted by the NASA Lewis code. Therefore a careful study of the amount of water generated by the gas generators was performed.

The gas samples that were taken from the two different gas generators during LAT tests and Plum Brook Station bag inflation tests (previous section) were determined as not reliable for water sample analysis. Difficulties were identified in the gas collection and handling that called into question the usefulness of a water content analysis on these samples. Therefore, ATK made special arrangements during a later LAT to condition the tank so as to ascertain the amount of water present inside the altitude tank after the

LAT. The results gave a more reliable means of determining the water vapor content of the generator exhaust by collecting all of the gases (as opposed to collecting a small sample of gases exiting the gas generator) and then conducting a condensation evaluation on this entire sample. To accomplish this evaluation the altitude tank was installed inside a thermal conditioning bay. By raising and lowering the LAT tank temperature and observing the internal pressure changes the amount of water that was undergoing phase change was easily calculated. The percentage of water present was determined to be 36.89% by volume, which is slightly higher than predicted by the Lewis code.

Benchmarking and Model Validation

The benchmarking and model validation of the airbag system model was accomplished by using six data sets to calibrate and tune the model. The model's developmental paths as accomplished through these six data sets are as follows:

1) Mars Pathfinder qualification test: This was a full-system inflation test. The MPF qualification data were used to compare the initial model's performance to program heritage by inspecting pressure, gas temperature, and fabric temperature profiles. This data set was used because there was no MER inflation data available at the initiation of the creation of the MER T&P model in May 2001. This data set was used as a baseline through the summer of 2001. The total grain mass in the gas generators during this test was 1.309 kg (0.421 kg boost grain).

2) Gas generator LAT at ATK tactical systems, 14 September 2001: The utility of the data from this test was to benchmark the model under simple and ideal boundary conditions. Additionally, ATK pulled samples from the inlet port of the LAT tank into sample cylinders for a post-test chemical analysis. The model achieved agreement with the measurements within 5% for a fixed volume and isothermal tank that was kept above the dew point (i.e., no condensation). This benchmark test was most critical in determining the number of moles (both condensable and noncondensable) that were being created by the gas generators. The total grain mass in the gas generators during this test was 1.452 kg (0.563 kg boost grain).

3) Single bag thermal vacuum inflation at the B-2 Facility at Plum Brook Station, 25 September 2001: This test used a gas generator containing 1.455 kg of grain mass (0.563 kg boost grain). This test gave the first opportunity to benchmark the T&P model with the dynamics of an inflation event and the complications associated with condensation and evaporation occurring on the interior bladder surface. Because a single bag was used the bag-to-bag venting was removed from the model and was not verified for accuracy. Also, this test used the MPF airbag design and the data were later determined not useful after the airbag design changed significantly to include an extra abrasion layer and a bladder restraint layer. However, good agreement with measurements (within 5%) for the gas pressure and temperature and the fabric temperature was achieved giving confidence in the model's thermodynamic behavior predictions.

4) Gas generator LAT test at ATK tactical systems, 1 April 2002: This test used a gas generator containing 1.266 kg of grain mass (0.383 kg boost grain). Although the main purpose of this test was a contractually required LAT, ATK provided useful data about the gas constituents created by the gas generators. ATK carefully conditioned the tank to estimate the amount of water vapor generated by the gas generators. Specifically, ATK observed the internal pressure inside the tank as the tank passed below and then above the dew point of the internal gas mixture. Using ideal gas relationships and the tank volume the number of water moles was computed. This test proved crucial in the estimation of the amount of water vapor deposited into the MER airbags during inflation. Model comparisons with measurements taken during the LAT tests for the gas pressure, gas temperature, and the derived moles are given in Figs. 4–6, respectively.

5) Full-system thermal vacuum inflation test in the B-2 facility at Plum Brook Station, 2 August 2002: This test is referred to as DM6A. The total grain mass in the gas generators during this test was 1.269 kg (0.419 kg boost grain). This test used the MER airbag

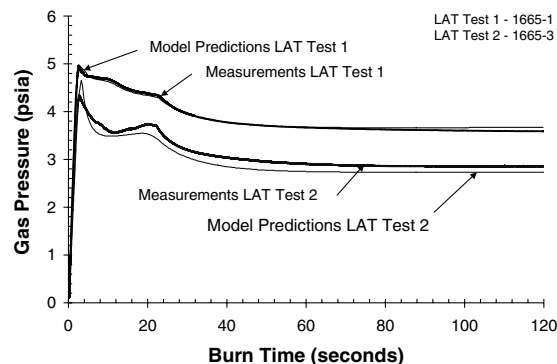


Fig. 4 Gas pressure benchmarking results for LAT tests.

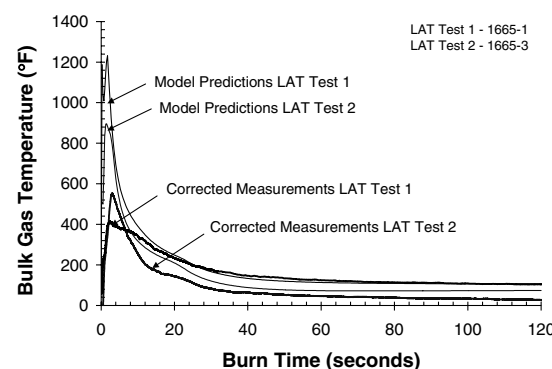


Fig. 5 Bulk gas temperature benchmarking results for LAT tests.

design and a gas generator with the MPF grain design minus 10% boost grain. Although an internal gage pressure of 1.0 psid (pound-per-square-inch-differential) was predicted the test produced only a maximum internal pressure of 0.8 psid. After a careful inspection of the data and the new airbag design it was determined, and verified by the T&P model, that the restraint layer was more thermally active with the internal gases than originally predicted. The added mass of the restraint layer was affecting the internal gases by lowering the temperature, and hence, the pressure. After the effect of this new mass was modeled more accurately from the DM6A data an updated boost grain size requirement was determined as the MPF baseline plus 25%. Because this was such a large change in boost grain size it was decided that a second inflation test in the B-2 facility was needed. This second full-system inflation test used the same DM6A airbags. However, rework had to be performed because a sequence of drop tests had been performed using these airbags before the second inflation test. Model comparisons with measurements taken during the DM6A tests for the gas pressure, gas temperature, the side bag fabric temperatures, and the bottom bag temperatures are given in Figs. 7–10, respectively.

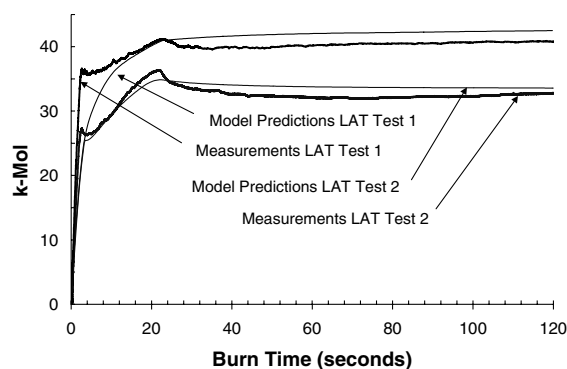


Fig. 6 Derived moles benchmarking results for LAT tests.

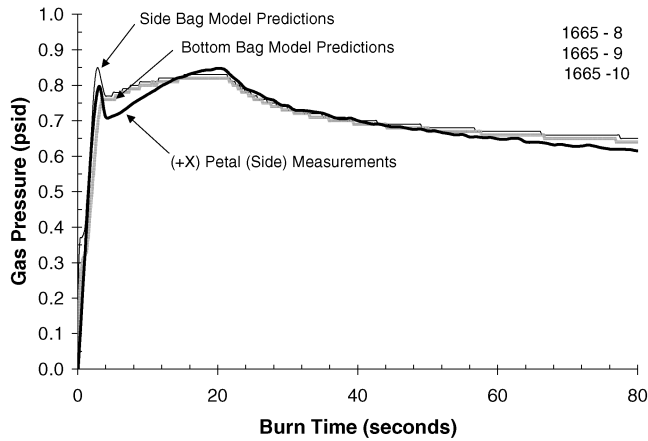


Fig. 7 Gas pressure benchmarking results for DM6A test.

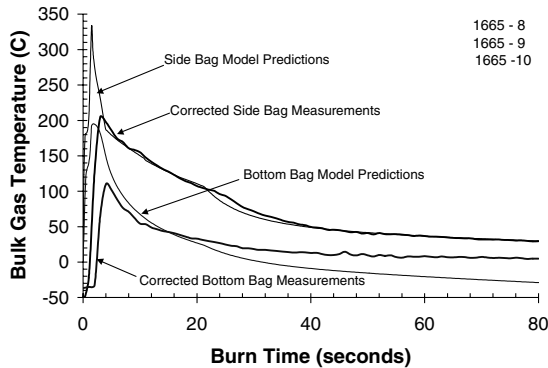


Fig. 8 Bulk gas temperature benchmarking results for DM6A test.

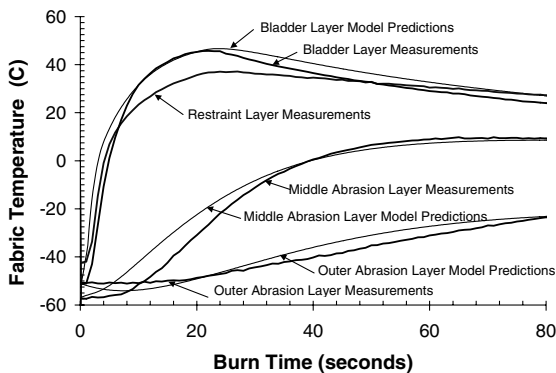


Fig. 9 Side bag fabric temperatures benchmarking results for DM6A test.

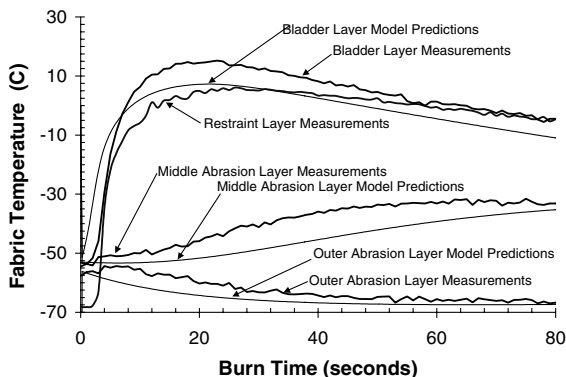


Fig. 10 Bottom bag fabric temperatures benchmarking results for DM6A test.

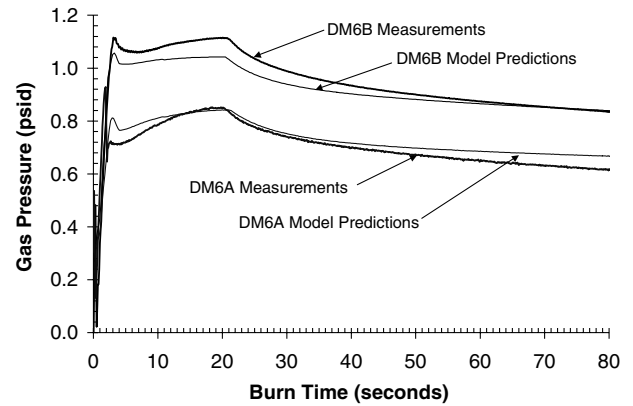


Fig. 11 Gas pressure benchmarking results for DM6A and DM6B tests.

6) Full-system thermal vacuum inflation test in the B-2 facility at Plum Brook Station, 10 December 2002: This test is referred to as DM6B. The total grain mass in the gas generators during this test was 1414 kg (0.525 kg boost grain). At the time of this test JPL system engineers had refined their mission analyses and all the airbag performance data from drop tests were available. The goal for the airbag system had been changed slightly to $1.0 + 0.0 / - 0.1$ psid. The results of this test gave a maximum pressure of 1.1 psid. The model had underpredicted the internal gas by 10% and a new and final benchmarking effort was undertaken. After slightly adjusting the amount of noncondensable gases coming from the gas generators the newly benchmarked model was used to finalize the boost grain size needed for the MER mission. After exercising the model in hot and cold mission scenarios it was determined that the flight grain configuration for MER should be the MPF baseline plus 20%. That is a total of 1.393 kg, with a boost grain of 0.504 kg. Model comparisons with measurements taken during both the DM6A and DM6B tests for the gas pressure, side bag gas temperature, and bottom bag gas temperature are given in Figs. 11–13, respectively.

MER Mission Predictions

The final benchmarked model was used to predict in-flight bag pressure during inflation for expected mission conditions for both extreme hot and cold environments. Figure 14 shows the predicted bag pressure profiles during landing and impact with the Mars surface for hot and cold mission scenarios, as described in Table 2. The bulk gas temperatures and fabric temperatures are not shown. Some general observations are made as follows:

- 1) A steady 1.0 psid pressure plateau is achieved up through almost the entire gas generator burn (22 s).
- 2) The impact of hot versus cold environments on the internal gas pressure is small for the first 80 s after the gas generators are fired. This is an expected result because there are six abrasion layers in

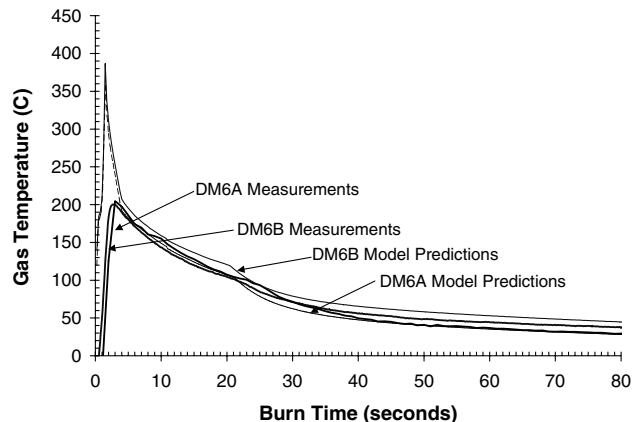


Fig. 12 Side bag bulk gas temperature benchmarking results for DM6A and DM6B tests.

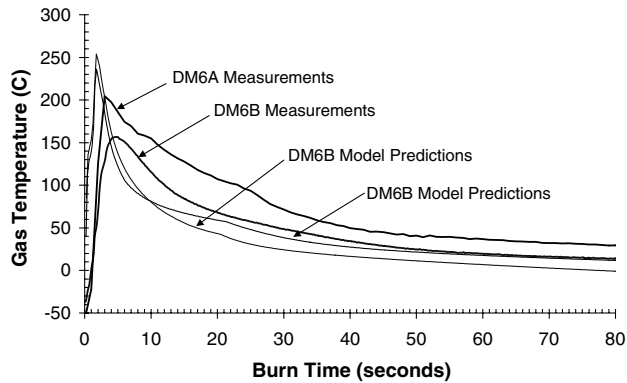


Fig. 13 Bottom bag bulk gas temperature benchmarking results for DM6A and DM6B tests.

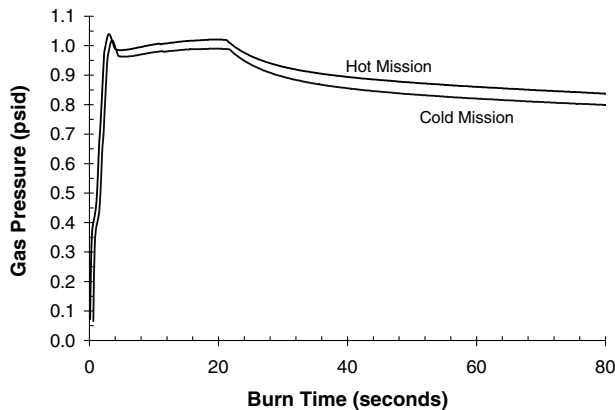


Fig. 14 Final mission bag pressure predictions for hot and cold mission scenarios.

addition to a restraint layer between the bladder layer and the outer Mars environment.

3) The initial bag temperatures at gas generator (GG) ignition (-45°C and -25°C for the cold and hot cases, respectively) are responsible for the small spread in the pressure profiles between the hot and cold mission scenarios.

4) Based on benchmarking results the predictions of in-flight pressures should be within a $\pm 5\%$ error band.

Final Comments

The Spirit rover landed on Mars on Saturday, 3 January 2004, and Opportunity rover landed on Saturday, 24 January 2004. With these two successful landings the airbag landing system developed by NASA has proved to be a viable option for direct impact landing systems.

Acknowledgments

The authors would like to thank Charlie Horton, President of GORCA Space and Communications, for his guidance, assistance, and leadership on this project. We would also like to thank the program managers at ILC Dover including Carl Knoll and George Sharpe who were both crucial to the success of this modeling program. Over a dozen JPL program engineers and managers participated in peer reviews and design reviews and gave critical insights and helpful engineering assistance including John Carson, Greg Davis, Siu-Chun Lee, Stephen F. Fuerstenau, Dara Sabahi, Adam Steltzner, and Rich Williamson.

References

- [1] Nguyen, H. T., and Wilson, D., "Thermal/ Pressure Modeling of the Mars Pathfinder Airbag System," AIAA Paper 98-2456, June 1998.
- [2] Incropera, F. P., and DeWitt, D. P., *Fundamentals of Heat and Mass Transfer*, 5th ed., Wiley, New York, 2002.
- [3] Mills, A. F., *Heat Transfer*, Irwin, Chicago, IL, 1995.
- [4] Ulrich, R. D., Wirtz, D. P., and Nunn, R. H., "Transient Heat Transfer in Closed Containers after Gas Injection," *Journal of Heat Transfer*, Vol. 91, 1969, pp. 461–463.
- [5] Weber, N., Rowe, R. E., Bishop, E. H., and Scanlan, J. A., "Heat Transfer by Natural Convection Between Vertically Eccentric Spheres," *International Journal of Heat and Mass Transfer*, Vol. 9, No. 1, 1966, p. 649.
- [6] Leckner, B., "Spectral and Total Emissivity of Water Vapor and Carbon Dioxide," *Combustion and Flame*, Vol. 19, No. 1, 1972, pp. 33–48.
- [7] Rohsenow, W. M., Hartnett, J. P., and Cho, Y. I., *Handbook of Heat Transfer*, McGraw-Hill, New York, 1998.

I. Vas
Associate Editor